Polymer 54 (2013) 2058–2061

Contents lists available at SciVerse ScienceDirect

Polymer

journal homepage: www.elsevier.com/locate/polymer

Polymer communication

Chemically imaging the effects of the addition of nanofibrillated cellulose on the distribution of poly(acrylic acid) in poly(vinyl alcohol)

Craig Clemons [a,*], Julia Sedlmair [a,b,c], Barbara Illman [a,b], Rebecca Ibach [a], Carol Hirschmugl [b,d]

[a] USDA Forest Service, Forest Products Laboratory, Madison, WI, USA
[b] Synchrotron Radiation Center, University of Wisconsin – Madison, Madison, WI, USA
[c] Department of Agricultural and Biological Engineering, The Pennsylvania State University, University Park, PA, USA
[d] Department of Physics, University of Wisconsin, Milwaukee, WI, USA

ARTICLE INFO

Article history:
Received 13 November 2012
Received in revised form
23 January 2013
Accepted 11 February 2013
Available online 18 February 2013

Keywords:
FTIR
Chemical imaging
Nanocellulose

ABSTRACT

The distribution of poly(acrylic acid) (PAA) in model laminates of nanocellulose and poly(vinyl alcohol) (PVOH) was investigated by FTIR chemical imaging. The method was effective in spatially discerning the three components of the composite. PAA can potentially improve the performance of nanocellulose reinforced PVOH by not only crosslinking the PVOH matrix but also improving the adhesion between PVOH and nanocellulose by forming ester linkages with both of them. However, PAA was found to migrate out of the PVOH matrix and concentrate in the nanocellulose layer of the laminate. This led to a PAA-depleted region in the matrix near the nanocellulose layer, which would likely lead to a weak interphase and limited stress transfer between the fiber and matrix in the heat-treated composite. Methods for improving the distribution of the PAA need to be investigated to optimize performance. This is the first chemical imaging study of nanocellulose materials using synchrotron-based vibrational spectroscopy.

Published by Elsevier Ltd.

1. Introduction

Polyvinyl alcohol (PVOH) has been investigated for use in a wide variety of applications such as controlled drug release hydrogels, separation membranes, fibers, and tissue engineering formulations [1,2]. For many applications, treatment of PVOH is required to render it more stable in water. This can be accomplished to some extent by heat-treating or by repeated freeze/thaw cycling but the most effective methods for long-term stability involve chemical crosslinking [2]. This is most often accomplished with mono- or di-aldehydes but recent investigations have explored the use of less toxic crosslinking agents such as poly(acrylic acid) (PAA) [1,2]. Ester linkages are formed between the hydroxyls of PVOH and the carboxyls of PAA during heat treating, which results in a network structure and renders the polymer insoluble in water.

PVOH has also been of interest as a matrix material for nanocellulose composites. Nanocellulose is a naturally-sourced reinforcement extracted from trees, plants, some marine creatures or certain bacteria and fungi [3]. Researchers are exploring a wide variety of uses of nanocellulose such as in dimensionally stable, optically transparent composites for flexible electronics [4] or in improved barrier membranes [2]. Types of nanocellulose, their properties, and their potential applications have been described in recent reviews [3,5,6]. Since its preparation most often results in aqueous dispersions, nanocellulose can be relatively easily dispersed in water-soluble polymers such as PVOH and then fabricated into composites. Several researchers have demonstrated mechanical property improvements when nanocellulose is added to PVOH [7–12]. Ultimately, however, their susceptibility to water and still modest mechanical performance limits the applications in which they can be used. Adding PAA to the PVOH during composite preparation may improve performance by not only crosslinking PVOH but also improving the adhesion between PVOH and nanocellulose by forming ester linkages with both of them. However, understanding and controlling this chemistry during fabrication is necessary for optimal performance.

Paraliker et al. [2] explored a PVOH-PAA-nanocellulose system. Fourier transform infrared (FTIR) spectroscopy showed ester formation with heat treatment and the composites with 80:10:10 PVOH:PAA:nanocellulose by weight yielded the highest mechanical performance. Follow-up work using atomic force microscopy (AFM) found gradients in the mechanical and adhesion properties of the interphase region between the nanocellulose surface and the bulk matrix suggesting variations in the densities of the ester linkages

* Corresponding author.
E-mail address: cclemons@fs.fed.us (C. Clemons).

0032-3861/$ – see front matter Published by Elsevier Ltd.
http://dx.doi.org/10.1016/j.polymer.2013.02.016

[13]. Optimization of this interphase region is crucial for effective stress transfer, especially since the large surface area of the nanocellulose means that much of the matrix is part of the interphase.

Determining the spatial distribution of the different components of the composite would be a useful step in understanding the behavior of these composites, especially in the critical region near the fiber–matrix interface. FTIR imaging can use the functional group chemistry of the composite constituents to image their spatial distribution. In this investigation, we used a new, synchrotron-based, mid-infrared beamline, IRENI (**I**nfra**R**ed **EN**vironmental **I**maging), at the University of Wisconsin Synchrotron Radiation Center (SRC) to image the PAA distribution in PVOH-PAA-nanocellulose composites. Laminates with layers of nanocellulose and matrix were used as model composites.

FTIR imaging is non-invasive and does not require staining or special sample environments. Comparing the single substances with the composites FTIR data gives information about the chemical interactions in the sample. Due to the unique design of the IRENI beamline it is possible to have truly diffraction limited resolution at all wavelengths in just a couple of minutes. The combination of visible and spectral information is crucial for investigating the distribution of the PVOH in the sample. Although FTIR spectroscopy is a common tool for studying polymers [14], such as wood polymers [15,16], IRENI rapidly generates data with higher sensitivity, spatial resolution, and signal to noise ratio. Previous studies on polymers [17], animal tissues [18], cultural heritage samples [19] and many other samples [20] have proven the capabilities of this instrument.

2. Experimental

The PVOH used had a molecular weight (M_W) of 85,000–124,000 and was over 99% hydrolyzed. The PAA had a M_W of 1800. Both polymers were obtained from Sigma–Aldrich and used as purchased.

The nanocellulose was a nanofibrillated cellulose (NFC), which was prepared using commercially-supplied fully bleached Eucalyptus pulp using a procedure similar to that of Saito et al. [21]. The pulp was carboxylated using 2,2,6,6-tetramethylpiperidinyl-1-oxyl (TEMPO), sodium chlorite and sodium hypochlorite as the oxidizing reactants at 60 °C for 48 h. The carboxylate content of the reacted pulp fibers was determined to be 0.46 mmol per gram of pulp via titration based on TAPPI Test Method T237 cm-98 [22]. Oxidized pulp fibers were then washed thoroughly with deionized water and refined in a disc refiner to break apart fiber bundles. The fiber slurry was diluted to facilitate separation of coarse and fine fractions by centrifuging at 12,000 g_f, and the coarse fraction was rejected. The nanofiber suspension was concentrated to a solid content of approximately 0.5% using an ultrafiltration system. A final clarification step was performed in which the nanofibril dispersion was passed once through an M-110EH-30 Microfluidizer (Microfluidics, Newton, MA) with 200- and 87-μm chambers in series. The NFC suspension was stored at 4 °C until use.

Cast NFC films were prepared by vigorously stirring the 0.5% NFC solution, de-aerating under vacuum, casting into a petri dish, and air-drying. For PVOH films, a 15% by weight aqueous solution was first prepared and then heated to 90 °C in a water bath and stirred for 30 min. The solution was de-aerated under vacuum, cast into a petri dish, and air-dried. FTIR analysis of pure PAA was performed on the original powder since the films made from it were extremely brittle.

Laminates were made by first preparing a PVOH solution as described above. Sufficient PAA was then added to yield a 2:1, 4:1, or 8:1 PVOH:PAA weight ratio. Each solution was de-aerated, cast into a petri dish and an NFC film was immersed in it. After air-drying, the final NFC layer and total laminate thicknesses were about 50 and 250 μm, respectively as measured by a calibrated optical microscope (Lietz Wetzlar). 10 μm thick cross-sections were cut from the films with a microtome and used for the FTIR analysis. Several of the microtomed laminate cross-sections were cross-linked by placing them on a hot plate at 170 °C for 45 min, which was found as optimal conditions for similar composites in previous work [2]. The spectra of these heat-treated laminates were normalized to that of the uncrosslinked laminates using the peak at 2942 cm^{-1}. This corresponds to the C–H stretch, which does not participate in the crosslinking reactions [1].

High-resolution FTIR images were recorded using the IRENI beamline at the University of Wisconsin–Madison Synchrotron Radiation Center (SRC), a national light source facility. The IRENI beamline is illuminated with storage ring radiation and equipped with a Bruker Hyperion 3000 FTIR microscope (Billerica, MA) A swath of radiation (320 mrad (horizontal) × 25 mrad (vertical)), is extracted from a bending magnet, collimated and rearranged into a matrix of 3 × 4 beams, by a set of mirrors. Slight defocussing at the sample position results in homogenous illumination at the sample plane, allowing for diffraction limited imaging of an area of 40 × 60 μm^2 over the whole spectral range (3800–850 cm^{-1}), with a spectral resolution of 4 cm^{-1} [18,23]. The microscope has a 74×, 0.65 Numerical Aperture (NA) objective with a condenser of matching NA. The FPA detector is a liquid nitrogen cooled Mercury Cadmium Telluride mid-IR detector with an array of 128 × 128 pixels that are recorded in parallel. The effective, projected sample pixel size at the FPA (focal plane array) detector is 0.54 μm^2. For each tile (34 × 34 μm^2 area) reported here, 64 × 64 $pixels^2$ were

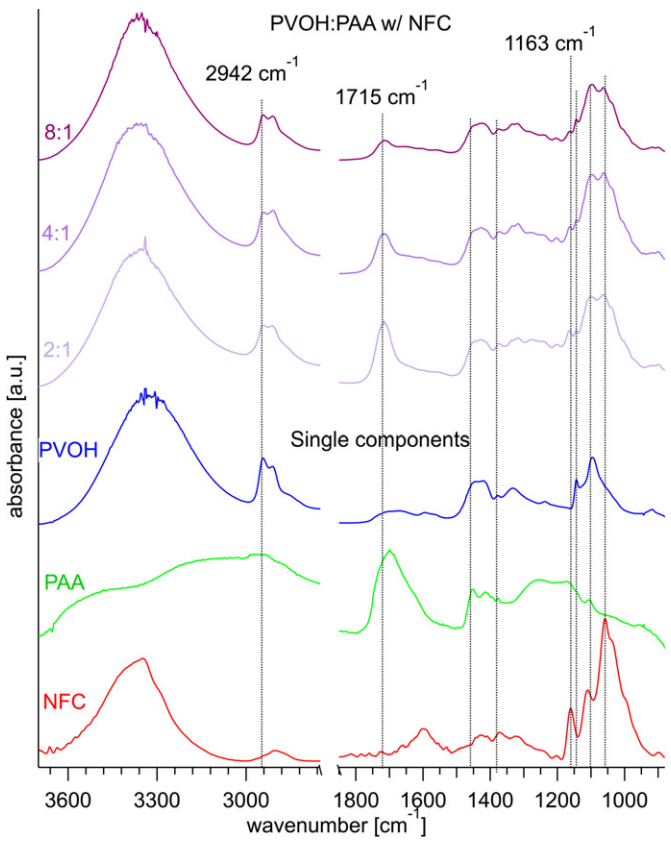

Fig. 1. FTIR spectra for pure PAA, PVOH, NFC, and the average spectrum of their composite. The selected absorption bands used for the integration images in Fig. 2 are indicated. More information is given in the text.

recorded simultaneously, and 256 scans were taken, for a total experimental time of 7 min/tile. The instrument has been described in detail elsewhere [20]. The following software programs were used for the analysis: OPUS (www.Bruker.com) and IRIDYS (www.iryidys.com), running on IGOR-PRO (www.wavemetrics.com).

3. Results and discussion

Fig. 1 shows the IR spectra of the pure components (bottom three plots) as well as the spectrum of the nanocomposite material (top plot) top, averaged over the entire sample area shown in Fig. 2. In order to identify each component within the composite, three absorption bands have been selected. These bands correspond to the C–H stretching in the PVOH around 2942 cm^{-1} [24], the C=O stretching in the PAA around 1715 cm^{-1} [25], and the C–O–C vibration (asymmetric) in the NFC around 1163 cm^{-1} [15]. The more specific limits used are 2928–2968 cm^{-1}, 1684–1759 cm^{-1}, and 1151–1181 cm^{-1} [16]. Additionally as guidance for the eye, vertical lines are drawn at specific absorption bands, characteristic for the individual materials to make it easier to compare features in the different spectra.

Fig. 2 displays the first chemical and spectral information obtained from IRENI on cellulose nanocomposites. Fig. 2a shows the visible light micrograph (VIS) of the cross section of the laminate. The central layer is the NFC layer with the modified PVOH polymer matrix on either side. The NFC map in Fig. 2b, integrated over the characteristic band for NFC at 1163 cm^{-1} clearly shows a discrete NFC layer (indicated in red) with little or no dispersion of the NFC in the matrix, indicating that the NFC film maintained its integrity during laminate preparation. Similarly, as seen in the integration image over 2942 cm^{-1} in Fig. 2d, the PVOH matrix (indicated in blue) forms discrete layers on either side of the NFC layer with only slight penetration into it. However, integration over 1715 cm^{-1} shows that PAA (green in Fig. 2c), is found in both regions. A significant PAA concentration is observable in the PVOH matrix far from the NFC layer (lower left portion of Fig. 2c), reflecting the PVOH-PAA blend prepared during laminate preparation. However, the PAA concentration decreases near the NFC layer and significant amount of PAA is found in the NFC layer itself. The migration of the PAA out of the matrix material and into the NFC layer resulted in a PAA-depleted region in the PVOH matrix near the NFC layer and suggests strong PAA-NFC interaction. Along the line scans indicated in Fig. 2b–d, 26 single point spectra were extracted and plotted in Fig. 2e, with the same spectral lines indicated as in Fig. 1. Following the changes of the peaks, these four regions, PVOH and PAA (purple), PAA-depleted PVOH (blue), interphase region (green), and PAA and NFC (ochre), are also identifiable by their spectral signature. In the left panel of Fig. 2f, the intensity profiles of the line scans (Fig. 2b–d) are shown, and illustrate that the observed layers are congruent. The four regions are also readily apparent.

The PAA distribution has major implications for the performance of such composites. The NFC scavenging of PAA would

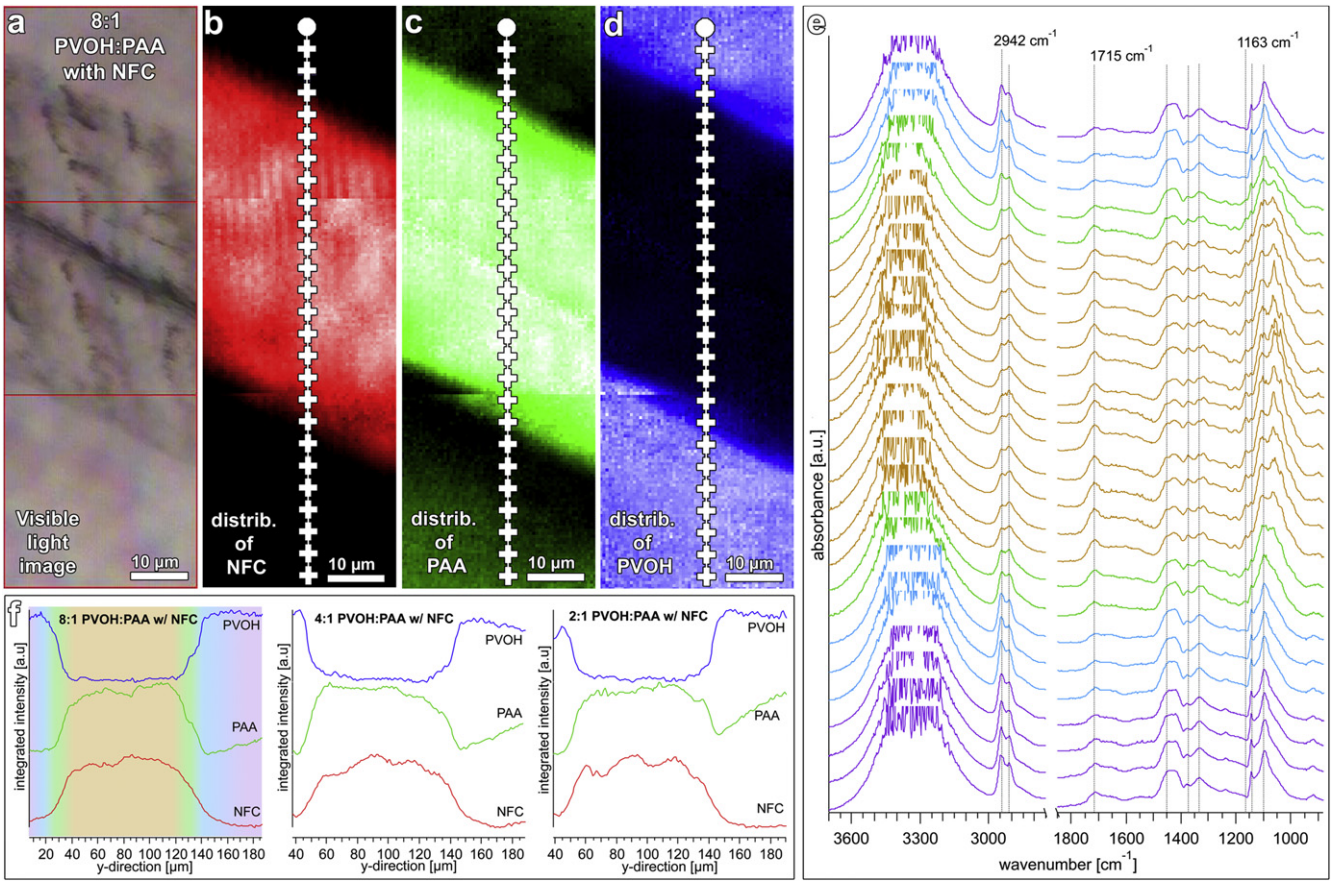

Fig. 2. Images of a PVOH:NFC laminate containing PAA demonstrating the different chemical compositions in the layers. An 8:1 PVOH:PAA weight ratio was used in Fig. 2a–e. Optical micrograph (a) and FTIR integration images: at 1163 cm^{-1} to show the distribution of NFC (b), at 1715 cm^{-1} for PAA (c), at 2942 cm^{-1} for PVOH (d). The color scales run from low (dark) to high (bright) concentration. The spectra of the line scans drawn in (b–d) are shown in Fig. 2e. As guidance for the eye, vertical lines have been drawn. Intensity profiles of the line scans from (b–d), showing the congruence of the layers in the integration images are shown in the left image of Fig. 2f. The other two images show the intensity profiles of similar line scans for laminates prepared with 4:1 and 2:1 PVOH:PAA weight ratios.

reduce the efficiency of PVOH crosslinking. Once heat-treated, the depleted region would result in a weak interphase region, limiting stress transfer between the nanocellulose and matrix. Also, this interphase region would be more easily affected by water because it is poorly crosslinked. If the nanocellulose was dispersed in the matrix rather than formed into layers as in our laminates, a greater portion of the matrix would likely be affected. More of the matrix would be in close proximity to the nanocellulose and susceptible to PAA scavenging. However, further investigation would be required to confirm this behavior.

The other two laminates with a ratio of 4:1 and 2:1 of PVOH:PAA have been analyzed in the same way and the intensity profiles of the line scans are also shown in Fig. 2f. The increase in PAA concentration in the PVOH matrix is readily apparent but the depleted region remains, indicating that a considerable amount of PAA can be scavenged from the PVOH by the NFC and simply adding more PAA would not offset this loss or result in a more uniform PAA distribution. Since a more even distribution of PAA would be preferable, methods for decreasing the mobility of the PAA by using higher solution concentrations during specimen preparation or a higher molecular weight PAA, for example, or controlling the interaction of the components by pH are being investigated.

Several laminates that were crosslinked by heat treating were also analyzed. During heat treatment ester linkages can be formed between the hydroxyls of PVOH or nanocellulose and the carboxyls of PAA resulting in a network structure [1]. Fig. 3 compares the average FTIR spectra for the initial and heat-treated laminates with 8:1 and 4:1 PVOH:PAA weight ratios. Because of its brittleness and high PAA content, a suitable cross section of the heat-treated laminate with a 2:1 PVOH:PAA weight ratio could not be prepared. Changes such as a reduction in the broad peak due to the hydroxyl groups in the 3000–3600 cm^{-1} range, a reduction in the shoulder around 1600–1650 cm^{-1}, and greater resolution of the peak at 1143 cm^{-1} with heat treatment are consistent with the findings of Paraliker et al. [2], who investigated similar treatments and composites. FTIR imaging of the heat-treated laminates yielded similar results as that of the untreated samples indicating that there was no spatial rearrangement of the composite components during heat treatment.

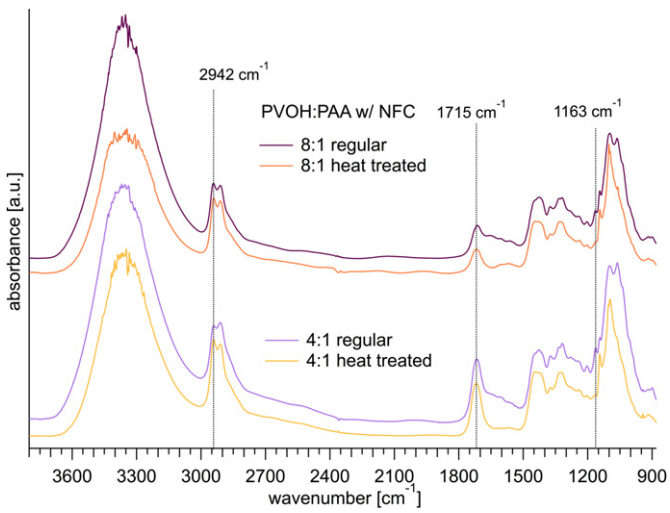

Fig. 3. Average FTIR spectra for initial and heat treated composites at different PVOH:PAA weight ratios.

4. Summary and conclusions

The distribution of poly(acrylic acid) (PAA) in model laminates of nanofibrillated cellulose (NFC) and poly(vinyl alcohol) (PVOH) was investigated by IRENI-FTIR chemical imaging. The method was effective in spatially discerning the three components of the composite. The PAA was found to migrate out of the PVOH matrix and into the nanocellulose layer of the laminate even at high ratios of PAA:PVOH. This led to a PAA-depleted region in the matrix near the NFC layer, which would likely lead to a weak interphase and limited stress transfer between the fiber and matrix in the heat-treated composite. Methods for improving the distribution of the PAA are being investigated to optimize performance.

Acknowledgments

The authors would like to acknowledge Rick Reiner of the Forest Products Laboratory for preparing and supplying the NFC. This work was partially funded by Agriculture and Food Research Initiative Grant no. 2011-67009-20056 from the USDA National Institute of Food and Agriculture and by U.S. Forest Service funds dedicated to nanotechnology research. This work was supported by the US National Science Foundation under awards CHE-1112433, and DMR-0619759, and is based on research conducted at the Synchrotron Radiation Center, University of Wisconsin–Madison, which is supported by the National Science Foundation under award DMR-0537588, and by the University of Wisconsin–Milwaukee and University of Wisconsin–Madison.

References

[1] Kumeta K, Nagashima I, Matsui S, Mizoguchi K. Journal of Applied Polymer Science 2003;90:2420–7.
[2] Paralikar SA, Simonsen J, Lombardi J. Journal of Membrane Science 2008; 320(1–2):248–58.
[3] Moon RJ, Martini A, Nairn J, Simonsen J, Youngblood J. Chemical Society Reviews 2011;40(7):3941–94.
[4] Nogi M, Handa K, Nakagaito AN, Yano H. Applied Physics Letters 2005;87:24.
[5] Eichorn SJ. Soft Matter 2011;7:303–15.
[6] Siró I, Plackett D. Cellulose 2010;17(3):459–94.
[7] Bhatnagar A. Journal of Reinforced Plastics and Composites 2005;24(12): 1259–68.
[8] Bruce D, Hobson R, Farrent J, Hepworth D. Composites Part A: Applied Science and Manufacturing 2005;36(11):1486–93.
[9] Lu J, Wang T, Drzal L. Composites Part A: Applied Science and Manufacturing 2008;39(5):738–46.
[10] Roohani M, Habibi Y, Belgacem N, Ebrahim G, Karimi A, Dufresne A. European Polymer Journal 2008;44(8):2489–98.
[11] Wang B, Sain M. Composites Science and Technology 2007;67(11–12): 2521–7.
[12] Zimmermann T, Pohler E, Geiger T. Advanced Engineering Materials 2004; 6(9):754–61.
[13] Pakzad A, Simonsen J, Yassar RS. Composites Science and Technology 2012; 72(2):314–9.
[14] Siesler HW, et al., editors. Near-infrared spectroscopy: principles, instruments, applications. Weinheim, Germany: Wiley-VCH; 2008.
[15] Pandey K. Journal of Applied Polymer Science 1999;71(12):1969–75.
[16] Fengel D. Das Papier 1992;46(1):7–11.
[17] Unger M, Mattson E, Schmidt Patterson C, Alavi Z, Carson D, Hirschmugl CJ. Applied Physics A 2012. http://dx.doi.org/10.1007/s00339-012-7481-6.
[18] Kastyak-Ibrahim MZ, Nasse MJ, Rak M, Hirschmugl C, Del Bigio MR, Albensi BC, et al. NeuroImage 2012;60(1):376–83.
[19] Echard JP, Cotte M, Dooryhee E, Bertrand L. Applied Physics A 2008;92(1): 77–81.
[20] Hirschmugl CJ, Gough KM. Applied Spectroscopy 2012;66(5):475–91.
[21] Saito T, Hirota M, Tamura N, Kimura S, Fukuzumi H, Heux L, et al. Biomacromolecules 2009;10(7):1992–6.
[22] TAPPI test method T 237 CM: carboxyl content of pulp. Norcross, GA: TAPPI Press; 1998.
[23] Nasse MJ, Walsh MJ, Mattson EC, Reininger R, Kajdacsy-Balla A, Macias V, et al. Nature Methods 2011;8(5):413–6.
[24] Smith BC. Infrared spectral interpretation: a systematic approach. Boca Raton, FL: CRC Press LLC; 1999.
[25] Dong J, Ozaki Y, Nakashima K. Journal of Polymer Science B: Polymer Physics 1997;35:507–15.